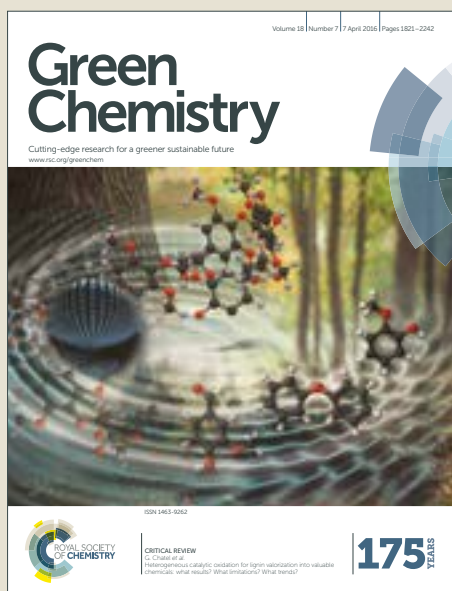


Green Chemistry

Accepted Manuscript



This article can be cited before page numbers have been issued, to do this please use: J. M. Carraher, T. Pfennig, R. G. G. Rao, B. H. Shanks and J. Tessonier, *Green Chem.*, 2017, DOI: 10.1039/C7GC00658F.



This is an Accepted Manuscript, which has been through the Royal Society of Chemistry peer review process and has been accepted for publication.

Accepted Manuscripts are published online shortly after acceptance, before technical editing, formatting and proof reading. Using this free service, authors can make their results available to the community, in citable form, before we publish the edited article. We will replace this Accepted Manuscript with the edited and formatted Advance Article as soon as it is available.

You can find more information about Accepted Manuscripts in the [author guidelines](#).

Please note that technical editing may introduce minor changes to the text and/or graphics, which may alter content. The journal's standard [Terms & Conditions](#) and the ethical guidelines, outlined in our [author and reviewer resource centre](#), still apply. In no event shall the Royal Society of Chemistry be held responsible for any errors or omissions in this Accepted Manuscript or any consequences arising from the use of any information it contains.



Green Chemistry

PAPER

cis,cis-Muconic acid isomerization and catalytic conversion to biobased cyclic-C₆-1,4-diacid monomers

Jack M. Carraher,^{a,b} Toni Pfennig,^{a,b} Radhika Giri Rao,^{a,b} Brent H. Shanks,^{a,b} and Jean-Philippe Tessonnier^{*,a,b}

Received 00th January 20xx,
Accepted 00th January 20xx

DOI: 10.1039/x0xx00000x

www.rsc.org/

Renewable terephthalic and 1,4-cyclohexanedicarboxylic acids can be produced from biomass via muconic acid using a combination of biological and chemical processes. In this conversion scheme, *cis,cis*-muconic acid is first obtained by fermentation using either sugar or lignin monomers as a feedstock. The diunsaturated *cis,cis*-diacid is then isomerized to *trans,trans*-muconic acid, reacted with biobased ethylene through Diels-Alder cycloaddition, and further hydrogenated or dehydrogenated to yield the desired 100 % renewable cyclic dicarboxylic acid. The isomerization of *cis,cis*- to *trans,trans*-muconic acid represents the main bottleneck in this process due to undesired side reactions that promote ring closing to form lactones. Therefore, new technologies for the selective isomerization of muconic acid are urgently needed. Here, we studied the corresponding reaction kinetics to elucidate the mechanisms involved in both the isomerization and cyclization reactions with the objective to identify conditions that favor the selective formation of *trans,trans*-muconic acid. We demonstrate that the reactivity of muconic acid in aqueous media strongly depends on pH. Under alkaline conditions, *cis,cis*-muconic acid is deprotonated to the corresponding muconate dianion. This species is stable for extended periods of time and does not isomerize. Conversely, *cis,cis*-muconic acid readily isomerizes to its *cis,trans*-isomer under acidic conditions. Prolonged heating further triggers the intramolecular cyclizations through reaction of the carboxylic acid and alkene functionalities. The formation of the muconolactone and its dilactone is kinetically favored over the isomerization to *trans,trans*-muconic acid over a broad range of conditions. However, strategies involving the chelation of the carboxylates with inorganic salts or their solvation using polar aprotic solvents were found to hamper the ring closing reactions and allow the isomerization to *trans,trans*-muconic acid to proceed with high selectivity (88 %). The obtained compound was further reacted with ethylene and hydrogenated to 1,4-cyclohexanedicarboxylic acid, an important monomer for the polyester and polyamide industries.

Introduction

Diacid monomers are central to the production of commodity polyamides and polyesters, a \$118bn market¹⁻³ with ties to the packaging and bottling, textiles, and automotive industries, among others.⁴ While these building blocks are typically manufactured from petroleum, the demand for renewable diacid monomers is increasing as a result of the growing number of environmentally-conscious end users.⁴⁻⁹ Significant efforts are, therefore, being dedicated to developing new processes to address this need. In the case of terephthalic acid (TPA), the common approach targets renewable *p*-xylene as a drop-in for oxidation in the AMOCO process (Scheme 1a).¹⁰⁻¹²

However, oxidation-free routes through muconic acid (MA), a platform intermediate from sugar and lignin fermentation,¹³⁻¹⁹ have also emerged (Scheme 1b). The MA route can be considered advantageous as this intermediate can be converted to a variety of commodity and specialty chemicals, including adipic acid,^{14, 19, 20} TPA,^{4, 5, 21} and 1,4-cyclohexanedicarboxylic acid (CHDA).²¹

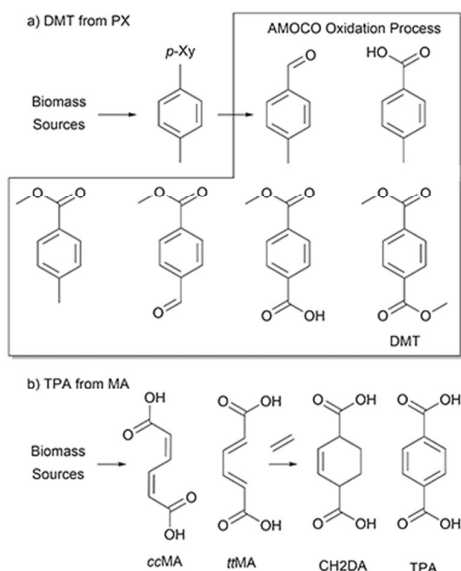
To access the cyclic products, MA is converted to 1,4-cyclohex-1/2-enedicarboxylic acid through Diels-Alder cycloaddition with ethylene, followed by dehydrogenation to TPA or hydrogenation to CHDA.^{4, 5, 21-25} So far, these research efforts have focused on the downstream conversion of the Diels-Alder active *trans,trans*-MA (*tt*MA) isomer. However, the preparation of cyclic diacids requires an additional MA isomerization step that has received little attention so far. There exists a significant gap in the literature with respect to isomerization of biologically-produced *cis,cis*-MA (*cc*MA) to Diels-Alder active *tt*MA.

While conceptually simple, the isomerization of MA to its *tt*- isomer was not reported until seven decades after the

^a Department of Chemical and Biological Engineering, Iowa State University, Ames, IA 50011, USA. E-mail: tesso@iastate.edu

^b NSF Engineering Research Center for Biorenewable Chemicals (CBiRC), Ames, IA 50011, USA.

† Electronic Supplementary Information (ESI) available: [details of any supplementary information available should be included here]. See DOI: 10.1039/x0xx00000x



Scheme 1. (a) Production of renewable terephthalic acid and its derivative dimethyl terephthalate (TPA) through stepwise oxidation of biobased *p*-xylene in the AMOCO process. Further hydrogenation yields the corresponding dimethyl 1,4-cyclohexanedicarboxylate. (b) Production of TPA and 1,4-cyclohexanedicarboxylic acid (CHDA) by isomerization of *cis,cis*- to *trans,trans*-MA, followed by Diels-Alder cycloaddition of ethylene, and de/hydrogenation.

initial publications on MA reactivity.²⁶⁻²⁸ It was in 1936 that the photocatalytic isomerization of MA in the presence of I₂ was described by Grundmann.²⁹ Still, two more decades passed until Elvidge *et al.* contributed a significant amount of work³⁰⁻³⁶ providing the first definitive identification of the much anticipated intermediate *cis,trans*-MA.³⁷ Following this pioneering work, it took another half century until Drath's corporation patented isomerization technologies utilizing catalysts such as Pd/C, and I₂ in acetonitrile under reflux or irradiation with UV light.^{4, 21, 23, 38-40} These findings, however, were not sufficient to propel the technology into the industrial realm. While noble metals are excellent de/hydrogenation catalysts, their high cost and relatively low selectivity in the isomerization to *tt*MA makes them less attractive for this step. Likewise, restrictions placed on the I₂ system, *e.g.* limiting feed solutions to 10 wt % MA, place serious economic constraints on the process. Finally, the low profit margins for high-volume-low-value chemicals like TPA only underscored these limitations.⁴ Conversely, low-volume-high-value chemicals like CHDA (\$5,000–10,000/ton vs. \$1,200/ton for TPA) would be more attractive. It would therefore be beneficial to the production of both TPA and CHDA to revisit the MA isomerization and develop green technologies for the economic production of *tt*MA.

To address this challenge, we chose to investigate the driving forces behind the spontaneous lactonisation of this molecule. This prompted us to seek a more in-depth understanding of MA's chemistry and gather insights that will facilitate new catalytic and non-catalytic isomerization routes. The current work is a mechanistic investigation into isomerization and lactonization of *cc*- and *ct*MA, respectively,

in an effort to understand the driving forces behind these reactions. Herein are described the spontaneous reactions of *cc*- and *ct*MA and the production of cyclic diacid monomers utilizing two new isomerization technologies directly resulting from this mechanistic study.

Results and discussion

A preliminary investigation of MA isomerization was carried out in which solutions containing 4.8 mM *cc*MA and 1.5 mM acetic acid (AA, used here as an internal standard) were heated to 75.5 ± 0.5 °C and monitored *in situ* by ¹H NMR (Fig. 1). Signals corresponding to *cc*MA (7.61 (2H) and 6.08 ppm (2H)) were consumed within approximately 20 minutes. Simultaneously, new signals (8.15, 6.82, 6.25, and 6.11 ppm, all 1H) corresponding to *ct*MA were observed. Further heating resulted in the loss of *ct*MA signals on significantly longer time scales, and the formation of singlets (7.83, 6.24, and 5.58 ppm, each 1H) and a pair of signals at 2.97 and 2.74 ppm (each 1H) attributed to muconolactone (Mlac). The pair of Mlac signals integrated to a single proton due to the incorporation of a solvent deuterium resulting in an undetectable signal (*vide infra*). Prolonged heating resulted in the appearance of two additional signals at 5.47 ppm (2H) and a pair of signals at 3.16 and 2.98 ppm (2H, 2H + 2D) assigned to tetrahydrofuro[3,2-*b*]furan-2,5-dione (Lac2).

Under these experimental conditions Mlac and Lac2 were found to be in equilibrium with the constant $K_{75\text{ }^\circ\text{C}} = 0.375$ (Fig. S1). These results revealed that the ring closing reactions are favoured over isomerization for *ct*MA. *tt*MA was not observed, which is consistent with the literature.^{4, 22-25, 37} A decrease in the amount of total signal as a function of time was observed and was attributed to the progressive incorporation of deuterium upon reversible lactonization to both Mlac and Lac2. This phenomenon is illustrated in Scheme S1. Kinetic traces for consumption of *cc*MA and *ct*MA fit first order rate equations (eq 1a), where $[ccMA]_t$ = concentration of *cc*MA at time *t*, $[ccMA]_\infty$ = concentration at time infinity,

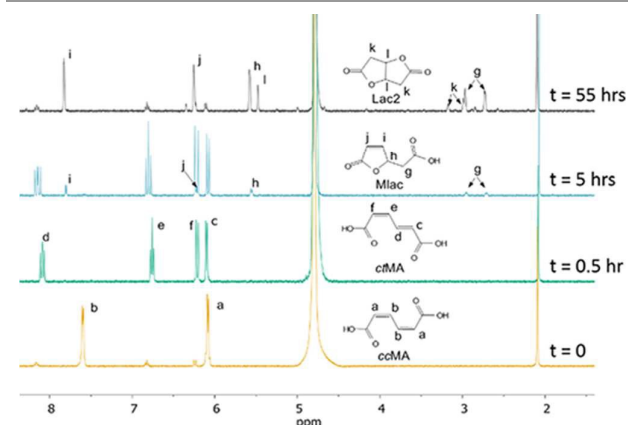
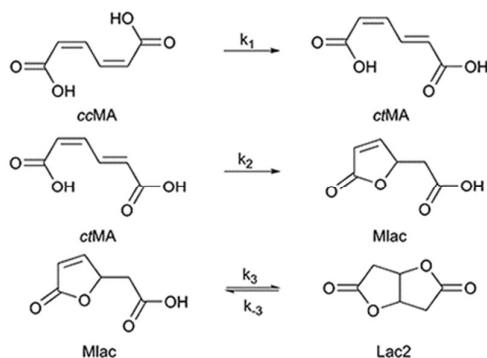


Figure 1. ¹H NMR spectra of muconic acid isomers (D₂O, 600 MHz, room temperature) with acetic acid internal standard (2.07 ppm). The large signal at 4.78 ppm is due to the solvent. Spectra are listed from bottom to top by increasing time intervals at 75 °C (t = 0, 0.5, 5, and 55 hours).



Scheme 2. Isomerization pathway used in KINSIM simulations shown in Figure 2. Scheme 2 does not consider pH effects.

$\Delta[\text{ccMA}] = [\text{ccMA}]_0 - [\text{ccMA}]_\infty$, k_{obs} = observed rate constant (s^{-1}), and t = time (s). As expected, increasing $[\text{MA}]$ had no effect on k_{obs} , consistent with the isomerization being first order with respect to $[\text{MA}]$. Kinetic simulations were performed using KINSIM utilizing the mechanism outlined in Scheme 2. The fit of simulated to experimental data shown in Figure 2a for the isomerization of ccMA to ctMA is excellent.

However, two key irregularities were observed for the further conversion of ctMA to Mlac and Lac2 (Fig. 2b). First, the experimentally determined concentrations of Mlac and Lac2 (and consequently $[\text{MA}]_{\text{total}}$) deviated from the simulations at long reaction times. At 50 and 75 °C, this was found to be due to incorporation of solvent deuterium and loss of proton in the reversible Mlac/Lac2 equilibrium described above (Scheme S1). This deviation became more pronounced at 95 °C, suggesting MA degradation. Second, the simulations deviated slightly from the experimental results for ctMA consumption at the beginning and end of the kinetic trace. The deviation at long reaction times can be accounted for by making corrections to the experimentally determined concentrations by the methods outlined in the ESI eqs. S1-S8 and demonstrated in Figures S2a-d. The latter observation suggested that pH affects the isomerization greatly, and this prompted a more in-depth investigation of pH effects on reaction kinetics.

$$[\text{ccMA}]_t = [\text{ccMA}]_\infty + \Delta[\text{ccMA}] \times \exp^{-k_{\text{obs}} \times t} \quad \text{eq 1a}$$

$$\ln([\text{ctMA}]_t / [\text{ctMA}]_0) = -k_{\text{obs}} \times t + \text{constant} \quad \text{eq 1b}$$

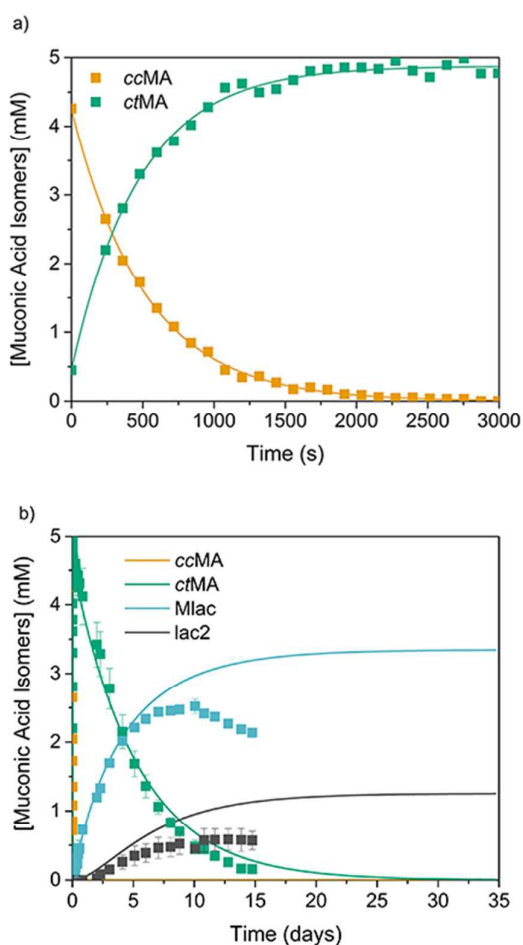


Figure 2. Experimental (■) and simulated (—) kinetic traces for ccMA isomerization at 83 °C (a) and ctMA isomerization at 75 °C (b)

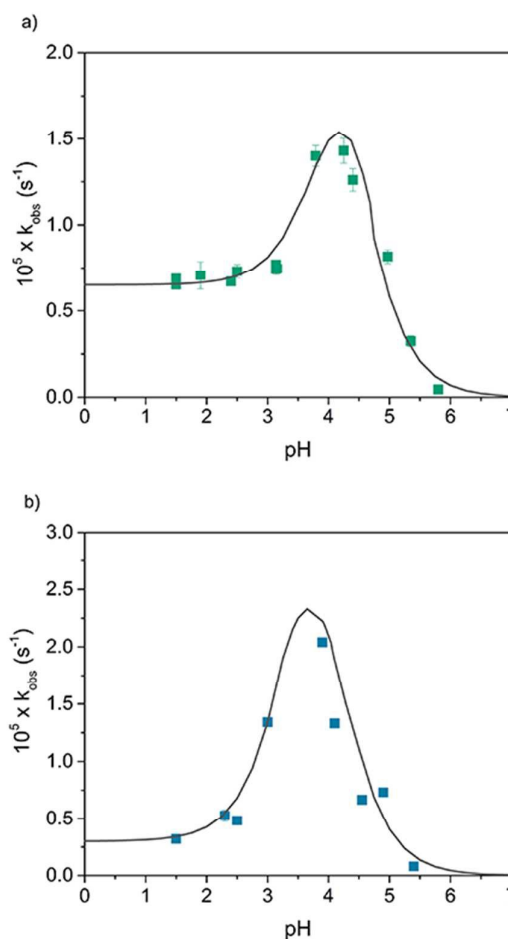


Figure 3. Plots of k_{obs} vs. pH for ccMA, 22.5 °C (top) and ctMA, 90.0 °C (bottom) conversion. (■) correspond to experimental data points; the line is only meant to guide the eye.

Effect of pH on reaction kinetics

Kinetic traces obtained over a wide range of pH values (1.7 to 6.5) fit first order rate equations (eq 1a for *ccMA* and the linearized form, eq 1b, utilizing the initial rates for *ctMA*). The dependence of k_{obs} on pH is shown in Figure 3 for both *ccMA* and *ctMA* conversions. It can be clearly seen that the observed rate constants were unaffected below $\text{pH} \sim 2.5$, increased between $\text{pH} 2.5$ and 4 to a maximum, then decreased between $\text{pH} 4$ and 6.5 to roughly 0 s^{-1} , i.e. no reaction was observed above $\text{pH} 7$. Figure 3 demonstrates why *E. coli* and *P. Putida* fermentations (typically carried out near neutral pH) report *ccMA* as the only isomer present.^{18,41}

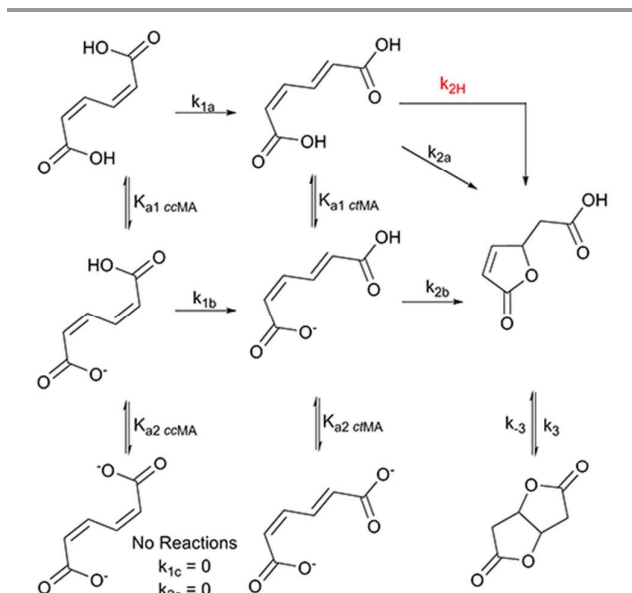
The trend in k_{obs} relative to pH can be explained by the reactivity of the various protonation states of MA. For instance, *ccMA* conversion at 22.5 °C (Fig. 3) occurred with a rate constant that was independent of pH up to 2.5 which is consistent with a unimolecular reaction of the fully protonated state (*ccMAH*₂). Between $\text{pH} 2.5$ and 4 the solution is primarily a mixture of *ccMAH*₂ and *ccMAH*⁺. Above $\text{pH} 4$ the solution is primarily a mixture of *ccMAH*⁺ and *ccMA*²⁻. Henceforth, the notation in this article will be MA for discussion of MA reactivity in general and *MAH*₂, *MAH*⁺, and *MA*²⁻ for specific protonation states. Scheme 3 was prepared with these considerations in mind.

Scheme 3 was simulated in KINSIM using the experimentally determined data in Table 1 and estimated values for parameters that were not directly measurable (eq S9-11 and Table S1). However, significant deviation of the model in Scheme 3 was observed for the low pH lactonization of *ctMA* at 50 °C (Fig. 4) and 75 °C due to an acid catalysed lactonization reaction pathway shown in equation 2. Therefore, values for $k_{2\text{H}}$ and $k_{2\text{a}}$ were determined in a series of experiments in which pH was less than 1.5 to ensure *ctMAH*₂ as the primary active species in solution. Plots of k_{obs} vs. $[\text{H}^+]$ were linear with y-intercept equal to $k_{2\text{a}}$ and slope equal to $k_{2\text{H}}$.

Table 1. Experimentally determined elementary rate constants and activation parameters for Scheme 3^a

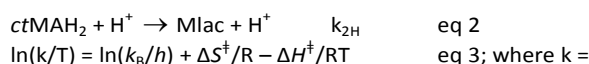
<i>ccMA-ctMA</i>	22.5 °C	50.0 °C	83.3 °C		ΔH^\ddagger (kJ/mol)	ΔS^\ddagger (j/molK)
$k_{1\text{a}}$	$6.5 \pm 0.6 \times 10^{-6}$	$9.5 \pm 1.0 \times 10^{-5}$	$1.5 \pm 0.3 \times 10^{-3}$		76 ± 1	-88 ± 2
$k_{1\text{c}}$	NR	NR	NR		NR	NR
<i>ctMA-Mlac</i>	50.0 °C	65.0 °C	75.0 °C	90.0 °C	ΔH^\ddagger (kJ/mol)	ΔS^\ddagger (j/molK)
$k_{2\text{a}}$	$8.0 \pm 1.0 \times 10^{-8}$	$5.2 \pm 0.5 \times 10^{-7}$	$1.5 \pm 0.1 \times 10^{-6}$	$3 \pm 1 \times 10^{-6}$	87 ± 11	-110 ± 34
$k_{2\text{c}}$	NR	NR	NR	NR	NR	NR
$k_{2\text{H}}^{\text{b}}$	$6.9 \pm 0.5 \times 10^{-6}$	$3.8 \pm 0.5 \times 10^{-5}$	$9.0 \pm 0.9 \times 10^{-5}$	NR	94 ± 5	-54 ± 13
<i>Mlac-Lac2</i>	50.0 °C	65.0 °C	75.0 °C	95.0 °C	ΔH^\ddagger (kJ/mol)	ΔS^\ddagger (j/molK)
k_3^{c}	$1.0 \pm 0.1 \times 10^{-7}$	-	$1.5 \pm 0.2 \times 10^{-6}$	1.5×10^{-5}	$98 \pm 1^{\text{d}}$	$-76 \pm 3^{\text{d}}$
k_{-3}^{c}	$2.4 \pm 0.5 \times 10^{-7}$	-	$4.0 \pm 0.8 \times 10^{-6}$	4.0×10^{-5}	$102 \pm 1^{\text{d}}$	$-56 \pm 2^{\text{d}}$
K_3^{c}	0.417	-	0.375	0.340	-	-

^a Experimentally determined rate constants (s^{-1}) and activation parameters for Scheme 3. Simulated results and estimations for acid dissociation constants and $k_{1\text{b}}$ and $k_{2\text{b}}$ are described in the ESI. 'NR' denotes 'no reaction' (i. e. $k = 0$), '-' corresponds to experiments that were not carried out under the specified conditions. ^b Second order rate constants for acid catalysed reaction ($\text{M}^{-1}\text{s}^{-1}$). ^c Values obtained from preliminary experiments near pH 3. No attempt was made to investigate pH effects on *Mlac* – *Lac2* equilibrium. ^d Activation parameters based on experiments near pH 3.



Scheme 3 Isomerization pathway accounting for pH effects. At 90 °C (Fig. 3b) the acid catalysed lactonisation pathway seen at lower temperature (Fig. 4), $k_{2\text{H}}$ (red), was not observed.

This pathway is active at elevated temperatures for reactions performed below $\text{pH} 2$ but its second order rate constant does not scale as rapidly with temperature as the unimolecular rate constant $k_{2\text{a}}$ (Table 1). Activation parameters were calculated for the individual steps with equation 3 and are also shown in Table 1. No attempt was made to determine the effect of pH on *Mlac*/*Lac2* equilibrium due to *ctMA*/*Mlac* irreversibility.



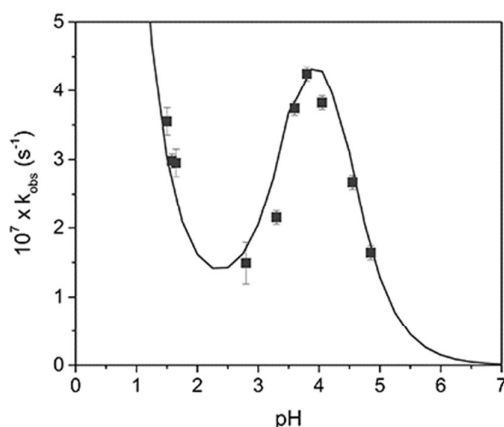


Figure 4. Plot of k_{obs} vs. pH for ctMA conversion at 50.0 °C. (■) correspond to experimental data points; the line is only meant to guide the eye.

elementary rate constant, T = temperature (K), k_B = Boltzmann constant, h = Planck's constant, ΔS^\ddagger = entropy of activation, and ΔH^\ddagger = enthalpy of activation.

Mechanistic information

The isomerization of *cc*MAH₂ (Scheme 4, reaction 1) appears to be dominated primarily by steric effects and solvent interaction with the transition state. Large values for the entropy of activation ($\Delta S^\ddagger = -88$ J/mol K) are typically observed in bimolecular reactions, but the isomerization of MA fits first order rate equations and k_{obs} is unaffected by [*cc*MA]. It is therefore reasonable to conclude it to be a unimolecular reaction. Solvent rearrangements to facilitate formation/stabilization of the transition state would explain the apparent discontinuity between these observations.

At higher pH, between 2.5 and 4, *cc*MAH₂ coexists with *cc*MAH⁻. We found that *cc*MAH⁻ isomerizes with a rate constant one order of magnitude larger than that of *cc*MAH₂. While steric interactions still likely play a role, the isomerization appears to be primarily driven by electronic interactions between the *cis*-carboxylate and its γ -C (Scheme 4, reaction 2 and Figure 5).

Above pH 4, the solution contains primarily *cc*MA²⁻, which remains stable for extended reaction times. Stabilization of *cc*MA²⁻ may be the result of resonance structures (Scheme 4, reaction 3) in which equal and opposite intramolecular carboxylate/ γ -C interactions stabilize the isomer. While these interactions appear to be strong enough to stabilize *cc*MA²⁻, no C-O bond formation to produce Mlac and Lac2 was observed. At no point was isomerization of *ct*MA to *tt*MA observed. Instead, lactonization occurred under all conditions below pH 7. The driving forces for lactone formation appear to be analogous to those for *cc*MA isomerization with two exceptions. First, *ct*MA ring closes *via* an acid catalysed pathway at low temperatures (Scheme 5, reaction 1) in addition to the unimolecular pathways shown in reactions 2a-b. Second, the lack of *ct*MA²⁻ reactivity cannot be explained by

a resonance structure in which the carboxylates exert an equal and opposite interaction with their respective γ -C atoms. Perhaps the lack of *ct*MA²⁻ reactivity can be explained by DFT calculations, but this is beyond the scope of the current work.

Like *cc*MAH₂, the kinetic traces for *ct*MAH₂ fit 1st order rate equations and k_{obs} did not vary with [*ct*MA], but the entropy of activation for *ct*MAH₂ lactonization was unusually large and negative for a unimolecular reaction. This again suggests a significant contribution from the solvent. It is unclear, however, if the reaction proceeds through pathway 2a or 2b of Scheme 5 or in a more concerted mechanism involving solvent as shown in Scheme 6. Reaction 3 of Scheme 5 may also be concerted like Scheme 6. Again, differentiation between these nuances may benefit from modelling by DFT, which is beyond the scope of the current work.

Though some questions with regard to fine detail remain, the kinetic behaviour indicates that there are two primary routes to consider if the goal is to prevent lactonisation and promote isomerization to *tt*MA. 1) Choosing a solvent that destabilizes the lactonisation transition state may promote *tt*MA formation. It is also preferable that *cc*- and *ct*MA have relatively high solubility to allow operation at higher reactant concentration. For this reason, polar solvents were chosen for the next part of this study (*vide infra*). Additionally, if Scheme 6

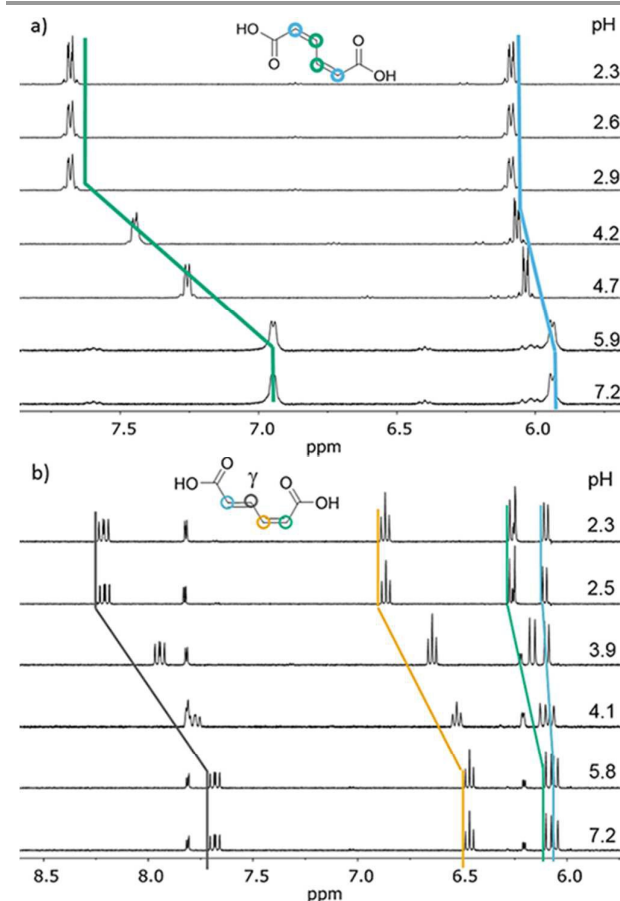
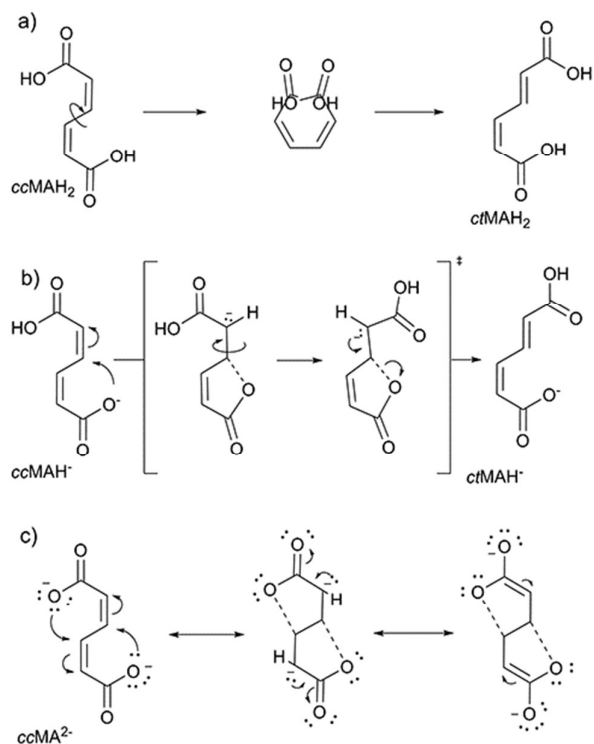


Figure 5. ¹H NMR spectra (D₂O, 600 MHz) of *cc*MA (a) and *ct*MA (b) in the pH range 2 – 7. The large change in chemical shift of the γ -C with pH supports a strong intramolecular interaction.

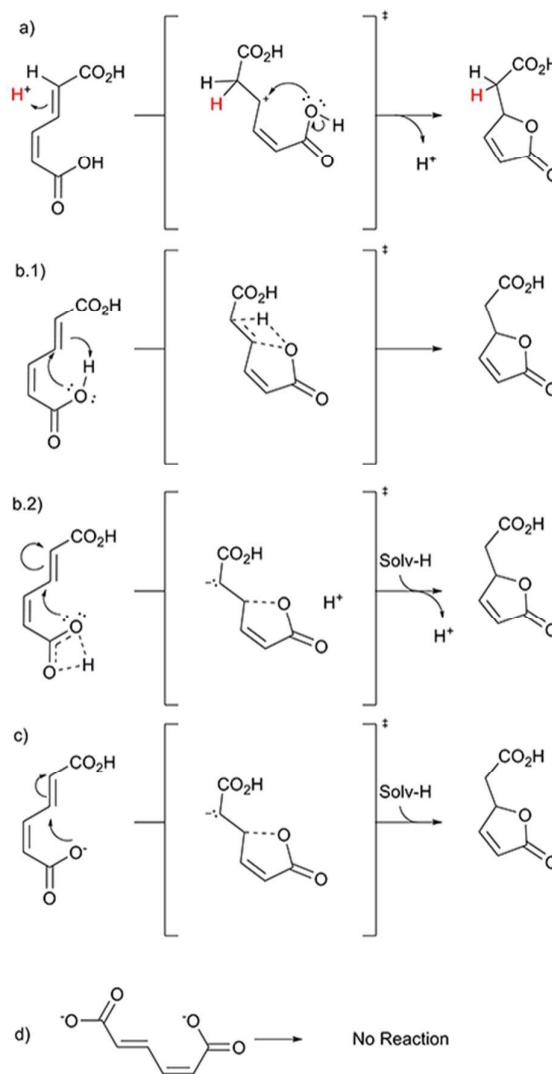


Scheme 4. Proposed mechanism for isomerization of *ccMA* at (a) low, (b) middle, and (c) high pH.

is an accurate representation of the role of water, *i.e.* proton exchange is required to facilitate lactonisation, then the solvent should also be aprotic. 2) The introduction of a species capable of binding carboxylate functionalities should disrupt the intramolecular interactions and allow for isomerization to *ttMA* as opposed to lactonisation. These hypotheses served as a basis for the work discussed in the next two sections.

Isomerization to *ttMA* in polar aprotic solvents

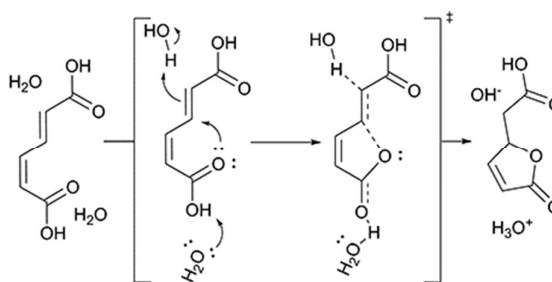
Results from a solvent screening in which primarily polar aprotic solvents were tested is summarized in Table 2. Toluene was the only non-polar solvent chosen in an attempt to identify the effect of polarity on the transition states in lactone formation vs. isomerization. This non-polar solvent did not yield any *ttMA*. All polar protic solvents yielded *Mlac* as the primary product (*ttMA* selectivity <5 %). This trend would support a lactonisation pathway outlined in Scheme 6. Noteworthy solvents are triethylamine, acetonitrile, and DMSO. Triethylamine is the only solvent in which severe degradation of *MA* was observed. That is, after 2 weeks at 75 °C no recognizable forms of *MA* (to include lactones) were observable. Acetonitrile yielded primarily lactones after 2 weeks. This is noteworthy in that it sheds more light on the role of the solvent, *vide infra*. THF and ethyl acetate yielded some *ttMA* (<5 %), but mainly formed lactones. DMSO was the only solvent in which *ttMA* was a major observable product. *ttMA* selectivity was as high as 88 % (62 % conversion) in DMSO. This observation offers interesting perspectives as



Scheme 5. Ring closing of *ctMA* to *Mlac* through acid catalysed reaction (a), and unimolecular isomerization at low (b), middle (c), and high pH (d).

DMSO is typically considered to be a green solvent.⁴²⁻⁴⁴

These results revealed that the role of the solvent is complex and cannot be simply described in terms of polar vs. nonpolar or protic vs. aprotic properties. At first glance, one could conclude that the polarity of the solvent would explain *Mlac* vs. *ttMA* reaction pathways, but if that were the case



Scheme 6. Possible solvent interaction facilitating lactonisation of *ctMAH₂*.

then toluene would be expected to yield *tt*MA, which it does not. Likewise, if it were a question of the solvents ability to donate/accept protons, then one would anticipate *tt*MA formation in acetonitrile. However, while acetonitrile is relatively polar and lacks the ability to donate protons, lactonisation dominates with no traces of *tt*MA. An investigation into the effects of solvent polarity on the molecular orbitals of *ct*MA and relative proton donating ability may provide useful insights into this phenomenon.

Isomerization to *tt*MA with inorganic salts

The above results suggest that successful isomerization to *tt*MA can be achieved by introducing a species that can bind the carboxylate and therefore minimize the intramolecular interactions that ultimately lead to lactonisation, specifically from *ct*MAH⁻. An obvious choice would be to operate at conditions under which the acids remain protonated. This would allow competition between Mlac and *tt*MA reaction pathways (Mlac has been shown to be unimolecular, *tt*MA is assumed unimolecular based on *cc*- and *ct*MA reaction pathways). However, the existence of the acid catalysed lactonisation pathway makes this route unfeasible as a low pH would be required. Additionally, no *tt*MA was observed at 90 °C (where the acid catalysed pathway is kinetically unobservable). Therefore, species with more electron withdrawing ability would be required.

A large number of metal ions can bind to carboxylates and hinder the undesired lactonization process.⁴⁵ Notably, aqueous lanthanum(III) exhibits large binding constants for carboxylates, typically on the order of 10³-10⁵.⁴⁵ A 20 mL solution of 5.1 mM *cc*MA was prepared in D₂O with an 89-fold excess of La_{aq}³⁺. The ¹H NMR is shown in Figure 6. The pD was adjusted to a pH reading of 4.34 (pD = 4.45)⁴⁶ with NaOH and HNO₃ in D₂O. After 5.8 days at 90 °C the conversion of *cc*MA was 75 % and *tt*MA was observed in 41 % yield (55 % selectivity); the solution was also composed of 14 % Mlac, 25%

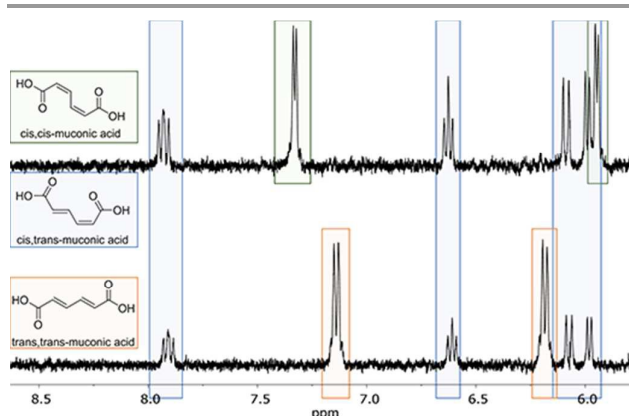


Figure 6. ¹H NMR (600 MHz, D₂O) spectra of 5.1 mM *cc*- & *ct*MA with 450 mM La(OH)₃ adjusted to pD = 4.45 with HNO₃ (top) was heated to 90 °C for 4 days (bottom).

*ct*MA, and the remaining 20 % were unidentified byproducts. Yields up to 55 % (60 % selectivity) were observed after 10.5 days at 75 °C. The selectivity varied widely with pH; up to 85 % near pH 5. At low pH (< 3) MA is present in the form MAH₂, which does not form a complex with La_{aq}³⁺ as well as MAH⁻ would. At high pH (> 5.5) La(OH)_n⁺⁽³⁻ⁿ⁾ species form; these species have a lower affinity for RCO₂⁻ and also lower solubility. Between these extremes (H₂O)_{4-n}La(OH)_nMAH_x^{+(3-n-x)} can form and a fraction of the La-MA complexes can precipitate. *tt*MA recovery, and catalyst recycling are described in more detail in the Supporting Information.

Production of 1,4-cyclohexanedioic acid

The further conversion of *tt*MA to CHDA was demonstrated through Diels-Alder cycloaddition of ethylene to *tt*MA in γ -valerolactone. The reaction resulted in the precipitation of cyclohex-1-ene-1,4-dicarboxylic acid (>99 % yield). The product was then esterified with methanol in the presence of H₂SO₄ due to solubility limitations for the subsequent hydrogenation reaction. Interestingly, esterification prior to Diels-Alder yielded cyclohex-2-ene-1,4-dimethyl ester in >94 % yield. The hydrogenation was then performed in a three-phase plugged flow reactor using Pt/C as a catalyst. The corresponding saturated ester (CHDAME₂) was obtained with 92 % yield at 97 % conversion.

Conclusion

A key hindrance to biorenewable CHDA and TPA from MA is the efficient isomerization of the biologically produced *cis,cis*-isomer to Diels-Alder active *trans,trans*-MA. In aqueous solutions *cc*MA readily isomerizes to *ct*MA which does not isomerize to *tt*MA, but instead produces Mlac. The driving forces for lactonisation are dependent upon pH. Below pH 2 the reaction is acid catalysed. Between pH 2 and 3 non-innocent interactions with the solvent drive lactonisation. Intramolecular interactions are responsible for lactonisation between pH 3 and 6, and above pH 6 the isomers are stabilized. Isomerization can be achieved by addressing the

Table 2. Isomerization Solvent Screening

Solvent ^a	Main Product
Acetone	Mlac
Toluene	Mlac
Acetonitrile	Mlac
THF	Mlac
Ethyl Acetate	Mlac
2-Propanol	Mlac
Triethylamine	Degradation
Methanol	Mlac
DMSO ^b	<i>tt</i> MA
Hexanol	Mlac

^a 3 ± 1 mg *cc*MA was added to 5 mL solvent, capped, and placed in an oven at 75 °C for 2 weeks. MA was recovered by rotary evaporation and re-dissolved in deuterium oxide for analysis by ¹H NMR. ^b DMSO-d₆ to eliminate the need for evaporation of solvent.

intramolecular interactions with aqueous lanthanum(III) salts. Strategies related to solvent driven lactonisation utilizing DMSO were also successful in producing *tt*MA. While the exact role of the solvent is unknown, it is clear that many solvents are non-innocent and their role in formation/stabilization of the transition states is non-trivial. A more in-depth study of MA reactions in DMSO would add significantly to our fundamental understanding of the reaction and to the development of economically viable industrial processes for the production of bio-derived monomers from muconic acid.

Experimental

Cis,cis-muconic acid (*cc*MA), *trans,trans*-muconic acid (*tt*MA), D₂O (99.9 % D), lanthanum hydroxide (La(OH)₃), acetic acid (AA), sodium perchlorate (NaClO₄), perchloric acid (HClO₄), trimethylamine, γ -valerolactone (GVL), and methanol (MeOH) were purchased from Sigma-Aldrich. Sodium hydroxide (NaOH), acetone, toluene, THF, ethyl acetate, 2-propanol, dioxane, and hexanol were purchased from Fisher. Ethylene 99.5 % was purchased from Airgas. DMSO-d₆ (99.96 % D) and acetonitrile-d₃ (99.96 % D) were purchased from Cambridge Isotopes Laboratories. All chemicals were used as purchased. *Cis,trans*-muconic acid (*ct*MA) was prepared by methods previously described in the literature.¹⁵

A base solution containing *cc*MA and AA (internal standard) was prepared in D₂O; separate solutions of HClO₄, NaOH, and NaClO₄ were prepared in D₂O. Aliquots of each solution were added to J. Young tubes, sealed, and placed in an oven. Samples were removed from the oven, cooled to room temperature, and analysed by ¹H NMR. Kinetic traces were constructed from MA signals relative to AA internal standard. Isomerization of *cc*MA to *ct*MA at either 75.5 or 83.3 °C required *in situ* ¹H NMR monitoring. Experiments in which pH effects were studied contained a 4-fold excess of AA as a buffer at higher pH (> 2.5).

Isomerization to *tt*MA with La(III) salts was carried out by dissolution of La(OH)₃ in HNO₃, addition of *cc*MA, AA internal standard, and adjusting pD to an appropriate range with NaOH and HNO₃ in D₂O. Solutions were heated in an oven at 90 °C for several days, and analysed by ¹H NMR.

¹H NMR spectra were collected with a Bruker AVIII600 spectrometer, and spectra were analysed with MestReNova software. *In situ* ¹H NMR kinetic spectra (75.5 or 83.3 ± 0.5 °C) were collected through a time-arrayed data set in which a single scan 1D proton spectrum was obtained at an interval of 12 seconds over the course of 30 minutes, and analysed with Bruker TopSpin3.2 software. The temperature for *in situ* studies was verified by ethylene glycol ¹H NMR temperature probe.⁴⁷ Data were plotted with OriginPro 9.1 software, and kinetic simulations were carried out with KINSIM kinetics simulation software.⁴⁸

Diels-Alder reactions of *tt*MA and ethylene were carried out in γ -valerolactone (acid) or methanol (ester) in a 50 ml batch micro reactor system (Parr 4590 Series). The reactor was sealed and purged with nitrogen to remove residual air, and charged with 500 psig ethylene until saturation of ethylene in

the solvent was reached. The temperature was then increased to 200 °C. After the reaction proceeded for the desired time (8-24 hrs), the reactor was cooled to room temperature and depressurized. The liquid phase reaction products were then collected, filtered through a cellulose filter dried, re-dissolved in DMSO-d₆ and analysed by NMR.

Hydrogenation of CH₂DAMe₂ was carried out in a stainless steel packed bed reactor using 10 mg of 5 wt % Pt/C catalyst diluted with 100 mg of glass beads (45-90 μ m). The reactor was operated in an upflow configuration at the temperatures of 250 °C. The temperature was maintained using a thermocouple and a PID controller. Reactions were conducted at hydrogen pressures of 8 bars. The gas flow rate was maintained at 20 ml/min using a Brooks SLA5850 flow controller. The reactant was dissolved in dioxane to obtain a concentration of 11.4 mg/ml. The liquid reactant feed was introduced in the reactor at a rate of 0.4 ml/min using an HPLC pump (Lab Alliance Series I). Product samples were collected every 15 minutes. The samples were dried overnight to evaporate the solvent. The dried samples were then dissolved in 600 μ l DMSO-d₆ and 1,3,5-tribromobenzene was added as an internal standard for analysis using ¹H NMR.

Acknowledgements

This material is based upon work supported in part by Iowa State University and the National Science Foundation Grant Number EEC-0813570. We gratefully acknowledge Mr. Bradley Schmidt of the Sadow group at Iowa State University for drying the DMSO-d₆, and the Iowa State University Chemical Instrument Facility staff members.

References

1. Polyamide Market by Type (PA 6, PA 66, Bio-Based & Specialty), by Application (Automotive, Films & Coatings, Industrial/Machineries, Consumer Goods & Appliances, Fibers & Textiles, and Others), by Process, and by Region - Global Trends and Forecast to 2020, <http://www.marketsandmarkets.com/Market-Reports/global-nylon-market-930.html>.
2. J. John, OpenPR homepage, 2016.
3. MarketsandMarkets, 2016.
4. D. I. Collias, A. M. Harris, V. Nagpal, I. W. Cottrell and M. W. Schultheis, *Industrial Biotechnology*, 2014, **10**, 91-105.
5. R. Lu, F. Lu, J. Chen, W. Yu, Q. Huang, J. Zhang and J. Xu, *Angewandte Chemie International Edition*, 2016, **55**, 249-253.
6. J. J. Pacheco and M. E. Davis, *Proceedings of the National Academy of Sciences*, 2014, **111**, 8363-8367.
7. Y. Tachibana, S. Kimura and K.-i. Kasuya, *Scientific Reports*, 2015, **5**, 8249.
8. R. A. F. Tomás, J. C. M. Bordado and J. F. P. Gomes, *Chemical Reviews*, 2013, **113**, 7421-7469.
9. B. S. Patrick, in *Green Polymer Chemistry: Biobased Materials and Biocatalysis*, American Chemical Society, 2015, vol. 1192, ch. 27, pp. 453-469.

10. C.-C. Chang, H. Je Cho, J. Yu, R. J. Gorte, J. Gulbinski, P. Dauenhauer and W. Fan, *Green Chemistry*, 2015.
11. H. J. Cho, L. Ren, V. Vattipalli, Y.-H. Yeh, N. Gould, B. Xu, R. J. Gorte, R. Lobo, P. J. Dauenhauer, M. Tsapatsis and W. Fan, *ChemCatChem*, 2017, **9**, 398-402.
12. C. L. Williams, C.-C. Chang, P. Do, N. Nikbin, S. Caratzoulas, D. G. Vlachos, R. F. Lobo, W. Fan and P. J. Dauenhauer, *ACS Catalysis*, 2012, **2**, 935-939.
13. K. A. Curran, J. M. Leavitt, A. S. Karim and H. S. Alper, *Metabolic Engineering*, 2013, **15**, 55-66.
14. D. R. Vardon, M. A. Franden, C. W. Johnson, E. M. Karp, M. T. Guarnieri, J. G. Linger, M. J. Salm, T. J. Strathmann and G. T. Beckham, *Energy & Environmental Science*, 2015, **8**, 617-628.
15. M. Suastegui, J. E. Matthiesen, J. M. Carraher, N. Hernandez, E. W. Cochran, Z. Shao and J.-P. Tessonier, 2015.
16. M. Suastegui and Z. Shao, *Journal of Industrial Microbiology & Biotechnology*, 2016, 1-14.
17. US5487987 A, 1996.
18. US 08/470,640, 1997.
19. W. Niu, K. M. Draths and J. W. Frost, *Biotechnology Progress*, 2002, **18**, 201-211.
20. J. E. Matthiesen, J. M. Carraher, M. Vasiliu, D. A. Dixon and J.-P. Tessonier, *ACS Sustainable Chem. Eng.*, 2016, **4**, 3575-3585.
21. US 12/816,742, 2013.
22. US 8,809,583, 2014.
23. WO2011085311A1, 2011.
24. USA Pat., US20130030215 A1, 2012.
25. US 8,426,639, 2013.
26. H. Limpricht, *Justus Liebigs Annalen der Chemie*, 1873, **165**, 253-302.
27. S. Ruhemann and F. F. Blackman, *Journal of the Chemical Society, Transactions*, 1890, **57**, 370-375.
28. F. Bode, *Justus Liebigs Annalen der Chemie*, 1864, **132**, 95-102.
29. C. Grundmann, *Berichte der deutschen chemischen Gesellschaft (A and B Series)*, 1936, **69**, 1755-1757.
30. U. Eisner, J. A. Elvidge and R. P. Linstead, *Journal of the Chemical Society (Resumed)*, 1953, 1372-1379.
31. J. A. Elvidge, R. P. Linstead, B. A. Orkin, P. Sims, H. Baer and D. B. Pattison, *Journal of the Chemical Society (Resumed)*, 1950, 2228-2235.
32. J. A. Elvidge, R. P. Linstead and J. F. Smith, *Journal of the Chemical Society (Resumed)*, 1952, 1026-1033.
33. J. A. Elvidge and P. D. Ralph, *Journal of the Chemical Society C: Organic*, 1966, 387-389.
34. J. A. Elvidge and P. Sims, *Journal of the Chemical Society C: Organic*, 1966, 385-387.
35. J. A. Elvidge, R. P. Linstead and P. Sims, *Journal of the Chemical Society (Resumed)*, 1953, 1793-1799.
36. J. A. Elvidge, R. P. Linstead and J. F. Smith, *Journal of the Chemical Society (Resumed)*, 1953, 708-711.
37. J. A. Elvidge, R. P. Linstead, P. Sims and B. A. Orkin, *Journal of the Chemical Society (Resumed)*, 1950, 2235-2241.
38. PCT/US2010/038792, 2013.
39. WO 2010078328 A3, 2010.
40. US 08/122,920, 2013.
41. WO2013092967 A1, 2013.
42. M. Martí, L. Molina, C. Alemán and E. Armelin, *ACS Sustainable Chemistry & Engineering*, 2013, **1**, 1609-1618.
43. F. P. Bryne, S. Jin, G. Paggiola, T. H. M. Petchey, J. H. Clark, T. J. Farmer, A. J. Hunt, C. R. McElroy and J. Sherwood, *Sustainable Chemical Processes*, 2016, **4**, 7.
44. W. Ghezali, K. De Oliveira Vigier, R. Kessas and F. Jerome, *Green Chemistry*, 2015, **17**, 4459-4464.
45. L. G. Sillen and A. E. Martell, *Stability Constants of Metal-Ion Complexes. Supplement No. 1. Pt.: Inorganic Ligands. Part 2: Organic Including Macromolecule Ligands. (Special Publication No. 25. Supplement No. 1 to Special Publication No. 17)*, Chem. Soc., 1971.
46. A. Krężel and W. Bal, *Journal of Inorganic Biochemistry*, 2004, **98**, 161-166.
47. G. De Wit, A. P. G. Kieboom and H. van Bekkum, *Carbohydrate Research*, 1979, **74**, 157-175.
48. B. A. Barshop, R. F. Wrenn and C. Frieden, *Analytical Biochemistry*, 1983, **130**, 134-145.